HHS Public Access

Author manuscript

Neuron. Author manuscript; available in PMC 2015 June 05.

Published in final edited form as:

Neuron. 2010 October 6; 68(1): 45–60. doi:10.1016/j.neuron.2010.08.013.

Nna1 Mediates Purkinje Cell Dendritic Development via Lysyl Oxidase Propeptide and NF-κB Signaling

Jianxue Li[1,*], **Xuesong Gu**[2], **Yinghua Ma**[6], **Monica L. Calicchio**[3], **Dong Kong**[2], **Yang D. Teng**[4,5], **Lili Yu**[7], **Andrew M. Crain**[8], **Timothy K. Vartanian**[6], **Renata Pasqualini**[9], **Wadih Arap**[9], **Towia A. Libermann**[2], **Evan Y. Snyder**[8], and **Richard L. Sidman**[1,*]

[1]Department of Neurology, Beth Israel Deaconess Medical Center

[2]Department of Medicine, Beth Israel Deaconess Medical Center

[3]Department of Pathology, Children's Hospital Boston

[4]Department of Neurosurgery, Brigham and Woman's Hospital

[5]Division of SCI Research, Veterans Affairs Boston Healthcare System Harvard Medical School, Boston, MA 02115, USA

[6]Department of Neuroscience and Neurology, Weill Medical College of Cornell University, New York, NY 10065, USA

[7]Department of Anatomy and Neurobiology, Boston University Medical School, Boston, MA 02118, USA

[8]Stem Cells and Regenerative Biology, Center for Neuroscience and Aging Research, Sanford-Burnham Medical Research Institute, La Jolla, CA 92037, USA

[9]David H. Koch Center, The University of Texas M. D. Anderson Cancer Center, Houston, TX 77030, USA

SUMMARY

The molecular pathways controlling cerebellar Purkinje cell dendrite formation and maturation are poorly understood. The *Purkinje cell degeneration* (*pcd*) mutant mouse is characterized by mutations in *Nna1*a gene discovered in an axonal regenerative context, but whose actual function in development and disease is unknown. We found abnormal development of Purkinje cell dendrites in postnatal pcd^{Sid} mice and linked this deficit to a deletion mutation in exon 7 of *Nna1*. With single cell gene profiling and virus-based gene transfer, we analyzed a molecular pathway downstream to *Nna1* underlying abnormal Purkinje cell dendritogenesis in pcd^{Sid} mice. We

*Correspondence: richard_sidman@hms.harvard.edu; jli7@bidmc.harvard.edu.

SUPPLEMENTAL DATA

Supplemental Data include six figures, five tables, experimental procedures, and references and can be found with this article online at http://www.cell.com/neuron/supplemental/

discovered that mutant *Nna1* dramatically increases intranuclear localization of lysyl oxidase propeptide, which interferes with NF-κB RelA signaling and microtubule-associated protein regulation of microtubule stability, leading to underdevelopment of Purkinje cell dendrites. These findings provide insight into *Nna1*'s role in neuronal development and why its absence renders Purkinje cells more vulnerable.

INTRODUCTION

Cerebellar Purkinje cells are central neurons controlling motor learning and coordination. Many fundamental concepts of modern neuroscience have been established by a focus on these vividly constructed cells (Rossi and Tempia, 2006). Three unique features make Purkinje cells a valuable model for the discovery of mechanisms underlying neuronal development and degeneration. First, Purkinje cells develop postnatally the most elaborate dendritic trees of all neurons in the human and rodent brain (Kapfhammer, 2004). Second, Purkinje cells are the most vulnerable neurons in various neurological diseases ranging from genetic defects to acquired injury or poisoning and from autism to Alzheimer's (Sarna and Hawkes, 2003). Third, Purkinje cells often undergo dendritic malfunction and cell death in circumstances that may cause lesser, but still debilitating, damage in other areas of the brain (Sirzen-Zelenskaya et al., 2006).

Since dendritogenesis is a key process in Purkinje cell development, essential for establishment of cerebellar circuitry, it is important to determine how developing Purkinje cell dendrites acquire their characteristic size and morphology (Wong and Ghosh, 2002). Development of Purkinje cell dendrites in postnatal cerebellum can be divided into two successive, tightly regulated stages. In the first postnatal week, bipolar fusiform Purkinje cells retract their primitive processes and extend numerous short perisomatic protrusions. In the second and third postnatal weeks, Purkinje cells form a primary dendrite and undergo rapid dendritic elongation and branching in the sagittal plane to elaborate their typical dendritic tree (Sotelo and Dusart, 2009). Although a number of genetic and environmental factors relate to cytoskeletal organization in Purkinje cells (Shima et al., 2004), the molecular pathways controlling dendrite formation and maturation, in contrast to axonogenesis, are poorly understood (Poulain et al., 2008). Purkinje cell dendrites are also abnormal in many diseases by mechanisms yet to be elucidated (Becker et al., 2009).

Here we characterized the *Purkinje cell degeneration* (*pcd*) mutant, pcd^{Sid} and uncovered an exon 7 deletion in *Nna1* (neuronal nuclear protein induced by axotomy). We then identified up-regulated lysyl oxidase (Lox) as a candidate molecule for dendritic underdevelopment of young pcd^{Sid} Purkinje cells. Lox is an extracellular copper enzyme that catalyzes conversion of lysine residues to aldehydes in collagen and elastin precursors, contributing to extracellular matrix formation and repair (Lucero and Kagan, 2006). Lox also plays diverse roles in developmental regulation of cardiovascular, pulmonary and cutaneous systems; and Lox-deficient mice die perinatally (Mäki, 2009). Although Lox increases in injured rat brain (Gilad et al., 2001), mutant SOD1 transgenic mouse brain (Li et al., 2004) and Alzheimer's disease human brain (Gilad et al., 2005), its modes of action in the central nervous system (CNS) are almost unknown.

With a set of complementary approaches, including primary Purkinje cell and organotypic slice cultures, neonatal cerebellar cortex injection, lentiviral vector-based cDNA or shRNA transduction, enzyme dynamics and dendritic tree quantification, we defined a molecular pathway leading to the dendritic underdevelopment. In this pathway, the *Nna1* mutation increases localization of Lox propeptide (a Lox fragment without enzymatic activity) in Purkinje cell nuclei, followed by inhibition of NF-κB RelA signaling, which further decreases microtubule-associated protein (MAP) 1B and MAP2, eventually suppressing Purkinje cell dendritic growth. NF-κB and MAPs were reported to regulate neuronal process outgrowth and migration (Gutierrez et al., 2005; Teng et al., 2001), and we further dissected their roles in postnatal development of Purkinje cell dendrites. This Lox-based metabolic pathway affects dendritogenesis, without an apparent effect on Purkinje cell viability.

RESULTS

Characterization of the *Nna1* mutation and Purkinje cell pathogenesis in *pcd^{Sid}* mutant mice

A spontaneous mutation was discovered in two mice in a litter of presumed wild-type BALB/c mice purchased from Charles River Laboratories. Ataxic progeny appeared in crosses of unaffected siblings with *pcd^{1J}* mice, and further breeding and histopathological analyses established that the mutation was allelic with *pcd*. It was named according to standard nomenclature procedures as *pcd^{Sid}* and has been maintained congenic with the C57BL/6J strain for more than 25 generations.

Homozygous *pcd^{Sid}* mutants showed reduced width of the cerebellar molecular layer and death of most Purkinje cells (Figures 1A-1I), resulting in severe ataxia, as in the previously described mutant alleles, *pcd^{2J-4J}* (Figures S1A-S1F) (Wang and Morgan, 2007). In *pcd^{Sid}* cerebella, all Purkinje cells were lost in lobules I-VIII between postnatal days 21 (P21) and P30, while some Purkinje cells in lobules IX-X survived for additional weeks. Unequivocal identification of *pcd^{Sid}* as an allele at the *Nna1* locus came from our evidence of an *Nna1* exon 7 deletion in cerebrum and cerebellum of *pcd^{Sid}* mutants, producing a stop codon in exon 8 (Figures 1J and 1K; Table S1). In addition, we characterized a six-nucleotide insertion between exons 6 and 7 of *Nna1* in *pcd^{4J}* brains (Figures S1G and S1H), in which a lysine at amino acid 176 was replaced by an isoleucine-lysine-glutamic acid tripeptide. Affected progeny also appeared in crosses between *pcd^{3J}* and *pcd^{4J}* heterozygotes.

To dissect the pathological process, we examined young *pcd^{Sid}* Purkinje cells prior to the onset of neuronal death and ataxia. In matings of *pcd^{Sid}* heterozygotes, P14 homozygous *pcd^{Sid}* progeny were distinguished from their heterozygous and wild-type littermates by accumulation of basal polyribosomes in Purkinje cell bodies (Figure 1L), suggesting early abnormalities in protein synthesis and processing (Landis and Mullen, 1978). In P20 *pcd^{Sid}* cerebellum, many Purkinje cells exhibited fewer dendritic branchlets in the molecular layer (Figure 2F), while some already showed the nuclear condensation and cytoplasm shrinkage typical of apoptotic cell death (Figure 1M) (Dusart et al., 2006). These findings suggest that the *Nna1* mutation in *pcd^{Sid}* may affect downstream molecules involved in at least three major functions: protein metabolism, dendritic growth and apoptosis.

Identification of molecules downstream from mutant *Nna1* in *pcd*^{Sid} Purkinje cells

The *pcd* disorder was recognized as Purkinje cell-autonomous by analysis of wild-type/*pcd* chimeras (Mullen, 1977), but available gene expression data in *pcd* mutants are neither comprehensive (Kyuhou et al., 2006) nor specific for affected Purkinje cells (Ford et al., 2008). Therefore, with laser capture microdissection (LCM) plus Affymetrix GeneChip array (microarray), we measured global gene expression in LCM-isolated individual Purkinje cell bodies and in LCM-isolated small groups of granule cells (Figures S2A-S2C; Table S2) from P20 *pcd*^{Sid} mutant and wild-type littermate cerebella. At this age, the pathological process had already begun, but most imperiled *pcd*^{Sid} Purkinje cells were still surviving.

We focused on candidate molecules whose expressions changed intensively in *pcd*^{Sid} Purkinje cells compared to wild-type Purkinje or granule cells and to *pcd*^{Sid} granule cells (Figure 2A). As verified by quantitative real-time PCR (qPCR) and gel identification (Figure 2B; Table S3), we discovered three candidate molecules, Calr3 (calreticulin 3), Lox and Bim (Bcl2-like 11), to be dramatically up-regulated more than 50-fold (Figures 2C and 2D). Because Calr3 is a molecular chaperone involved in protein synthesis and processing (Bedard et al., 2005), and Bim functions as a neuronal apoptosis facilitator (Greene et al., 2007), the up-regulation of Calr3 and Bim expression may be responsible, respectively, for abnormal protein metabolism (Figure 1L) and neuronal death (Figure 1M) in young *pcd*^{Sid} mutants, leading to Purkinje cell death (Figure 2G). Thus, in the present study, we have addressed a probable role of excess Lox in regulating postnatal growth of Purkinje cell dendrites.

By measuring spatial and temporal expression of Lox with qPCR, we found Lox mRNA levels (over the base line at 2% of Gapdh) to be detectable in most areas of wild-type mouse embryonic CNS, in about half the sampled areas of P7 CNS, and in fewer areas of adult CNS (Figure S2D), suggesting that Lox expression decreases with CNS development and maturation. With Western blot and immunohistochemistry, we also found Lox protein levels to be relatively low in P7-P20 wild-type cerebella, but increased in P20 *pcd*^{Sid} cerebella (Figure 2E) and Purkinje cells (Figure 2F), concurrent with the reduced dendritic branching (Figure 2F). Importantly, the above changes were also found in *pcd*^{2J} mutants (Figures S1I-S1K).

Suppression of Purkinje cell dendritic growth *in vitro* by Nna1 shRNA or Lox cDNA

We set up mixed cultures of primary cerebellar cells from P0 mouse pups (Figure S3A), in which cultured Purkinje cells came to resemble postnatal Purkinje cells *in vivo* by forming dendritic branchlets (Figures 3A and 3B) through two stages (Tabata et al., 2000). To establish an *in vitro* model of the *pcd* Purkinje cell pathological process, we transduced wild-type cerebellar cell cultures with lentiviral vector-based Nna1 shRNA (Table S5) from 7 to 14 days *in vitro* (DIV), and found that Nna1 RNA interference (RNAi) significantly suppressed Purkinje cell dendritic growth at 14 DIV (Figures 3C and 3D) and increased Purkinje cell death at 21 DIV (Figure S3B). We also co-transduced cerebellar cell cultures with both Nna1 shRNA and Lox shRNA (Table S5), and found that Lox shRNA greatly rectified Nna1 RNAi-reduced Purkinje cell dendritic growth (Figures 3C and 3D), but did

not prevent Nna1 RNAi-triggered Purkinje cell death (Figure S3B). These results suggest that Lox plays a role in *pcd* Purkinje cell dendritic development, but is less important in *pcd* Purkinje cell death.

To verify the possible relationship between increased Lox and abnormal dendritic development, we treated cerebellar cell cultures with suramin, a Lox expression stimulator (Buchinger et al., 2008), and found that suramin suppressed Purkinje cell dendritic growth (Figures 3E and 3F). We then transduced cerebellar cell cultures with lentiviral vector-based Lox cDNA (Figure S3C; Table S5) from 2 to 7 DIV (the early stage), or from 7 to 14 DIV (the later stage), and found that Lox cDNA significantly reduced Purkinje cell perisomatic sprouting at the early stage (Figure S3D) and Purkinje cell dendritic arborization at the later stage (Figures 3E, 3F and S3E), which were rectified by Lox shRNA (Figures 3E and 3F). The efficiency of Lox cDNA or Lox shRNA transduction was confirmed by Lox protein assay in either cultured cells or culture medium (Figure 3G). These results suggest that increased Lox expression in cerebellar cell cultures may interfere with Purkinje cell dendritic growth at both early and later stages.

We next set up cerebellar organotypic slice cultures (Li et al., 2006a,b) from P7 mouse pups (Figure S4A) to analyze later stages of Purkinje cell dendritic growth (Figures 4A and 4B) and viability (Figure S4B). We found that treatment with suramin or Lox cDNA from 0 to 7 DIV (P7 + 7 DIV = 14 days) and from 10 to 14 DIV (P7 + 14 DIV = 21 days) greatly suppressed Purkinje cell dendritic growth (Figures 4C and 4D; data not shown). These effects on Purkinje cell dendrites could be rectified by Lox shRNA (Figures 4C and 4D), and were coincident with our finding that Lox up-regulation *in vivo* was accompanied by underdevelopment of P20 *pcd* Purkinje cell dendrites (Figures 2F, S1I and S1K).

Verification of Lox cDNA effects on Purkinje cell dendritic development *in vivo*

Viral vectors carrying the L7 promoter are useful for selective expression of a foreign gene in Purkinje cells *in vivo*, but this promoter's low transcriptional efficiency and large size limit its value for transduction (Takayama et al., 2008). Lentiviral vectors have a larger insert capacity, elicit no or minimal inflammatory response, and integrate genes into target cell chromosomes, leading to stable long-term expression (Hirai, 2008; Torashima et al., 2006). To avoid an inhibitory effect on Purkinje cell dendrites caused by a strong MSCV (murine stem cell virus) promoter (Sawada et al., 2010), we prepared lentiviral vector-based gene constructs carrying the weaker CMV (cytomegalovirus) promoter (Table S5). These constructs themselves did not change Purkinje cell dendrite morphology *in vivo* (Figure 5E).

To study whether excess Lox affects postnatal development of Purkinje cell dendrites *in vivo*, we injected Lox cDNA tagged with eGFP, control eGFP cDNA, or control vehicle into the cerebellar cortices of P7 wild-type mice (Figure S5A; Table S5). As expected, the locally transduced Purkinje cells displayed green fluorescence (Figure S5B), and Lox cDNA significantly suppressed development of Purkinje cell dendrites examined at P14 and P21 (Figures 5A-5E). However, this inhibitory effect on dendritic development did not lead to the Purkinje cell death (Figures S5C and S5D), characteristic of *pcd* mutants at P21-P28. Lox cDNA and control cDNA also transduced a small number of granule cell precursors, stellate or basket interneurons, and Bergmann glial cells, but these cells did not show

obvious changes in morphology (Figures S5E-S5G). These *in vivo* results thus confirm our *in vitro* findings that excess Lox interferes selectively with Purkinje cell dendritic arborization during postnatal development.

Inhibitory effect of excess Lox on Purkinje cell dendrites is cell-autonomous and independent of Lox enzymatic activity

To test whether the effect of excess Lox on Purkinje cell dendritic growth is cell-autonomous, we transduced P0 enriched Purkinje cell cultures with Lox cDNA, and then added either P7 enriched granule cells or 7 DIV conditioned medium from cerebellar cell cultures into the transduced Purkinje cell cultures. We found that Lox cDNA did suppress dendritic growth of the enriched Purkinje cells, and this was not prevented by addition of enriched granule cells or conditioned medium (Figures 6A and 6B), suggesting that over-expressed Lox may affect Purkinje cell dendritic growth in a cell-autonomous manner, independent of neighboring granule cell actions and factors in the conditioned medium.

To check whether the inhibitory effect of excess Lox on Purkinje cell dendritic growth is related to Lox enzymatic activity, we treated cerebellar cell cultures with various Lox enzyme regulators. We verified that copper (a Lox enzymatic activator) and Lox cDNA increased Lox enzymatic activities (Figure 6C), while bathocuproinedisulfonate (BCS, an inhibitor of extracellular Lox activity) and β-aminopropionitrile fumarate (BAPN, an inhibitor of both extracellular and intracellular Lox activity) (Erler et al., 2006) not only inhibited Lox enzymatic activities, but also restored Lox cDNA-increased enzymatic activities (Figure 6C). However, neither copper nor BCS and BAPN changed the morphology of Purkinje cell dendritic trees, or prevented Lox cDNA-suppressed Purkinje cell dendritic growth (Figures 6D and 6E). These findings were also confirmed in wild-type cerebellar slice cultures (Figures 4C and 4D). Thus, we found no significant correlation between Lox enzymatic activity and Purkinje cell dendritic growth (Figure 6F).

Furthermore, we treated pcd^{Sid} (Figures 4C and 4D) and pcd^{2J} (Figures S4C and S4D) cerebellar slice cultures with BCS, BAPN or Lox shRNA, and found that only Lox RNAi prevented *Nna1* mutation-triggered abnormal Purkinje cell dendritic growth at the later stage. Nonetheless, Lox cDNA did not significantly change Purkinje cell survival in wild-type control slices (Figures S4E and S4F), and Lox RNAi or enzymatic inhibitors did not rectify Purkinje cell loss in pcd^{Sid} slice cultures (Figures S4E and S4F). Survival of granule cells (Figure S4G) and glial cells (Figure S4H) did not differ among the various treatments. These slice culture experiments verify our findings with the cerebellar cell cultures, i.e., Lox RNA knockdown, rather than Lox enzymatic inhibition, can rectify *Nna1* mutation- or Nna1 shRNA-suppressed Purkinje cell dendritic development, but this does not prevent *pcd* Purkinje cell death.

Excess Lox propeptide in Purkinje cell nuclei is responsible for Purkinje cell dendritic underdevelopment

We next looked more deeply into the basis for the effect on Purkinje cell dendritic development by analyzing Lox propeptide. Lox is synthesized as a ~50 kDa precursor, secreted into the extracellular matrix, and subsequently catabolized to a 30 kDa mature

enzyme fragment from the C-terminal moiety and an 18 kDa propeptide fragment without enzymatic activity from the N-terminal region (Lucero and Kagan, 2006). Extracellular Lox propeptide is arginine-rich, and readily taken up by cells due to its unusually high isoelectric point of 12.5 (Palamakumbura et al., 2004). We transduced cerebellar cell and slice cultures with lentiviral vector-based Lox propeptide cDNA (Table S5), whose efficiency was confirmed by Lox propeptide protein assay (Figure 6G). We found that Lox propeptide cDNA by itself did not change Lox enzymatic activity (Figure 6C), but like Lox cDNA, did suppress Purkinje cell dendritic growth in both cerebellar cell (Figures 6D and 6E) and slice (Figures 4C and 4D) cultures. These results confirm that excess Lox or Lox propeptide suppresses Purkinje cell dendritic growth by mechanisms unrelated to Lox enzymatic activity.

Since Lox and Lox propeptide are known to display stage-dependent distribution in various organelles of osteoblasts (Guo et al., 2007), we measured Lox and Lox propeptide distribution in Lox cDNA- or Lox propeptide cDNA-transduced Purkinje cells, where dendritic growth was suppressed. The two primary antibodies we used were an antibody against the C-terminal segment of Lox for detecting entire Lox or Lox enzyme, and a Lox propeptide antibody against the N-terminal segment for detecting entire Lox or Lox propeptide. We found that no signals could be detected by either antibody in control Purkinje cells (Figure 6H). When Purkinje cells were transduced by Lox cDNA, the signals were detected in nuclei, cell bodies and dendrites by the Lox enzyme antibody, and were detected in nuclei and cell bodies by the Lox propeptide antibody (Figure 6H). When cells were transduced by Lox propeptide cDNA, the signals were detected predominantly in nuclei by only the Lox propeptide antibody (Figure 6H). These findings indicate that excess Lox propeptide protein is concentrated in Purkinje cell nuclei, a site for gene transcriptional regulation.

Nna1 shRNA or Lox propeptide cDNA suppresses Purkinje cell dendritic growth via reduced RelA

Lox and Lox propeptide were reported to suppress cancer cell transformation (Palamakumbura et al., 2004) or vascular smooth muscle cell proliferation (Hurtado et al., 2008) via inhibition of NF-κB signaling. Because NF-κB regulates neuronal process outgrowth (Gutierrez et al., 2005) and synaptic function (Meffert et al., 2003), we hypothesized that the inhibitory effect of excess Lox propeptide on Purkinje cell dendrites might be mediated by abnormal NF-κB signaling. Our microarray and qPCR data showed that RelA, a major member of the NF-κB family, was significantly down-regulated in LCM-isolated *pcd*^{Sid} Purkinje cells (Figures 2A and 2B). We also measured three components (Table S3) of the NF-κB family in Nna1 shRNA-, Lox cDNA- or Lox propeptide cDNA-transduced cerebellar cell cultures, and found that mRNA and protein levels of NF-κB RelA were greatly decreased, while NF-κB p50 and IκBα were not significantly changed (Figures 7A and 7B). Importantly, we observed that Lox RNAi could rectify Nna1 shRNA-induced NF-κB RelA reduction (Figures 7A and 7B).

We next checked effects of diverse Nna1 and RelA treatments on Lox levels, and found that Nna1 shRNA, rather than RelA cDNA or shRNA, significantly increased Lox mRNA levels

in cultured Purkinje cells (Figure 7C). Also, neither RelA cDNA nor shRNA rectified the Nna1 shRNA-induced Lox mRNA up-regulation (Figure 7C). The efficiency of RelA cDNA or shRNA transduction was verified by RelA protein assay (Figure 7D). Furthermore, both Lox and RelA manipulation did not change Nna1 expression (data not shown).

RelA contains a transactivation domain that is required for transport of the active NF-κB complex into cell nuclei. In contrast, p50 lacks this domain and must form heterodimers with RelA to translocate into cell nuclei. We observed by immunohistochemistry and confocal microscopy that intranuclear RelA was much lower in P20 *pcd*^{Sid} mutant Purkinje cells than in wild-type controls *in vivo* (Figure 7E). With DNA-binding ELISA assays we measured NF-κB activation in Purkinje cell nuclei, and found that RelA over-expression increased only RelA transactivation (Figure 7F), but not p50 transactivation (Figure 7G), while RelA down-regulation by Nna1 shRNA, Lox cDNA, Lox propeptide cDNA or RelA shRNA significantly inhibited both RelA (Figure 7F) and p50 (Figure 7G) transactivation.

We found further that RelA down-regulation suppressed Purkinje cell dendritic growth (Figures 7H and 7I). To detect whether abnormal RelA mediated excess Lox-suppressed dendritic growth of Purkinje cells, we treated Lox cDNA-transduced cerebellar cell cultures with an NF-κB activator, tumor necrosis factor-α (Royuela et al., 2008), and found that this factor significantly protected Purkinje cell dendritic trees (data not shown). In addition, although RelA cDNA by itself did not obviously alter Purkinje cell dendritic morphology (Figures 7H and 7I), it did rectify Nna1 shRNA- or Lox propeptide cDNA-suppressed Purkinje cell dendritic growth (Figures 3C, 3D, 6D, 6E, 7H and 7I), suggesting that NF-κB RelA down-regulation mediated the inhibitory effects of Nna1 RNAi or Lox propeptide over-expression on dendritic growth of developing Purkinje cells.

Abnormal NF-κB signaling alters MAPs controlling Purkinje cell dendritic growth

Microtubules composed of tubulin subunits are major cytoskeletal components running longitudinally in neuronal processes, and MAPs bind to tubulin subunits to control microtubule stability. MAP-microtubule binding is regulated by microtubule affinity regulating kinase (MARK) with phosphorylation detaching MAP from microtubules. We detected a significant down-regulation of MAP1B mRNA and MAP2 mRNA, and an up-regulation of MARK3 mRNA in LCM-isolated Purkinje cells of P20 *pcd*^{Sid} mutants (Figure S6A). Both MAP1B and MAP2 are expressed predominantly in Purkinje cell dendrites, relative to Purkinje cell axons (Chauhan and Siegel, 1997). The double knockout of MAP1B and MAP2 has synergistic effects on neuronal migration, dendritic growth and microtubule organization (Teng et al., 2001). We examined spatial and temporal distribution of microtubule and MAP proteins in postnatal cerebella by immunohistochemistry, and found obvious decreases of MAP1B, MAP2 and tubulin βIII in the molecular layer of P20 *pcd*^{Sid} cerebellar cortices (Figure 8A). We next measured MAP1B and MAP2 in cerebellar cell cultures that had been transduced by Nna1 shRNA, Lox cDNA, Lox propeptide cDNA or RelA shRNA, and found that these lentiviral vector-mediated transductions inhibited MAP1B and MAP2 levels in Purkinje cell dendritic branches (Figure 8B). Furthermore, we found by quantitative analysis that Lox shRNA or RelA cDNA rectified Nna1 RNAi-reduced MAP1B, while RelA cDNA rectified Lox or Lox propeptide cDNA-reduced

MAP1B (Figure S6B). These results indicate that changes in microtubule and MAP levels are associated with Purkinje cell dendritic underdevelopment in postnatal *pcd* cerebellar cortices *in vivo* and in Nna1 shRNA-treated cerebellar cell cultures.

To establish a causal relationship between abnormal MAP levels and Purkinje cell dendritic underdevelopment, we transduced cerebellar cell cultures with MAP shRNA and cDNA. Neither MAP1B shRNA nor MAP2 shRNA alone changed Purkinje cell dendritic trees, but a joint application of the two shRNAs significantly suppressed Purkinje cell dendritic growth (Figures 8C and 8D). In contrast, either MAP1B cDNA or MAP2 cDNA individually rectified RelA shRNA-suppressed Purkinje cell dendritic growth (Figures 8C and 8D). These data are consistent with a previous report (Teng et al., 2001), suggesting a functional redundancy between MAP1B and MAP2, and a synergistic effect of their double deficiency on Purkinje cell dendritic growth. Our findings disclose that abnormal MAP1B and MAP2 mediate the underdevelopment of Purkinje cell dendrites triggered by *Nna1* mutation, Lox-propeptide cDNA or RelA shRNA.

DISCUSSION

In this study, we characterize a *pcd* mutant allele, pcd^{Sid} that shows postnatal Purkinje cell death and severe ataxia due to the deletion of *Nna1* exon 7. We correlate increased Lox with underdevelopment of pcd^{Sid} Purkinje cell dendrites prior to neuronal death, and dissect a molecular pathway (Figure 8E) in which the *Nna1* mutation up-regulates Lox and increases Lox propeptide in Purkinje cell nuclei. The excess Lox propeptide inhibits NF-κB RelA signaling and MAP roles in Purkinje cell dendritic growth. We formulate this molecular pathway based on several findings. First, the *Nna1* mutation increases Lox, reduces RelA and MAPs, and suppresses Purkinje cells dendritic growth *in vivo* and *in vitro*, supporting that Lox, RelA and MAPs are downstream from Nna1. Second, although excess Lox reduces RelA, manipulation of RelA does not alter Lox levels, suggesting that RelA is downstream from Lox. Third, RelA shRNA alters MAPs and suppresses Purkinje cell dendritic growth, while MAP cDNA blocks the inhibitory effects of RelA shRNA on Purkinje cell dendritic growth, an indication that MAPs are downstream from NF-κB RelA signaling.

The *pcd* mouse model (Wang and Morgan, 2007), one of the first among the presently identified ~50 mutation-induced cerebellar ataxias, includes a group of autosomal recessive mutations in the *Nna1* gene, $pcd^{1J\text{-}8J,Babe,Btlr,Tg}$. We present two previously-undescribed *Nna1* mutations: a deletion of the entire exon 7 in pcd^{Sid}, and a six-nucleotide insertion between exon 6 and exon 7 in pcd^{4J}, further evidence that *Nna1* is a vulnerable gene. We also report that P20 pcd^{Sid} mutants feature Purkinje cell dendritic underdevelopment just before the onset of massive Purkinje cell loss.

Global gene profiling in entire cerebellum does not provide the spatial resolution to address malfunction of Purkinje cells selectively, and conventional microarray strategies may not accurately analyze a very little RNA (<1 ng) from single cells. To gain a more comprehensive view of the molecular relationships involved in pcd^{Sid} Purkinje cell pathogenesis, we develop an advanced strategy of pico RNA amplification and cDNA purification followed by microarray to measure the global gene profiling in LCM-isolated

P20 wild-type and *pcd*^{Sid} Purkinje cells and granule cells. At P20, although molecular pathogenic changes have begun, *pcd*^{Sid} Purkinje cells are still surviving. We not only identify up-regulated candidate molecules such as Calr3, Lox and Bim for abnormal protein synthesis, dendritic underdevelopment and apoptosis, respectively, but also disclose additional potential markers for Purkinje cells and granule cells (Table S2).

Lox has been widely described to have multiple roles in formation and repair of extracellular matrix (Lucero and Kagan, 2006), in development of cardiac, pulmonary and cutaneous tissues (Mäki, 2009; Rodríguez et al., 2008; Szauter et al., 2005), and in tumor progression and metastasis (Erler et al., 2006; Payne et al., 2007). Although Lox levels are increased in selected types of diseased brains in rodents and humans (Gilad et al., 2001, 2005; Li et al., 2004), its role in the CNS is unknown. Here, we describe a pathological role of excess Lox in the CNS, particularly in Purkinje cell dendritic development. We show that the remarkably up-regulated Lox levels in *pcd*^{Sid} Purkinje cells are concurrent with *pcd*^{Sid} Purkinje cell dendritic underdevelopment, and that excess Lox negatively regulates dendritic arborization of developing Purkinje cells in cerebellar cell or slice cultures and in the cerebellar cortex *in vivo*.

Most of the previously reported effects of Lox involve its copper-utilizing enzymatic activity, particularly on extracellular collagen and elastin. In contrast, nonenzymatic Lox propeptide suppresses prostate (Palamakumbura et al., 2009), breast (Min et al., 2007), lung and pancreatic (Wu et al., 2007) cancer cells. We observe that Purkinje cell dendritic growth is suppressed by excess Lox via mechanisms independent of its enzymatic activity, for Lox enzymatic inhibitors do not rectify actions of Lox over-expression, and Lox propeptide (lacking Lox enzymatic activity) has a similar action to enzymatic Lox. Thus, our study prompts a new research direction on this important molecule.

Lox propeptide inhibition of cancer cell transformation and tumor formation is associated with NF-κB and other signaling pathways (Min et al., 2007; Palamakumbura et al., 2009; Wu et al., 2007). In the CNS, nuclear translocation and gene activation of transcription factor NF-κB regulate neuronal processes (Gutierrez et al., 2005) and synapses (Meffert et al., 2003). We find that excess Lox propeptide suppresses Purkinje cell dendritic growth also via the NF-κB signaling pathway. RelA, a major member of the NF-κB family and a positive regulator of neuronal process growth, shows reduced expression and less nuclear translocation in *pcd*^{Sid} Purkinje cells *in vivo*. A role for RelA in this dendritic development pathway is also consistent with the observed down-regulation of RelA expression and inhibition of RelA transactivation by Nna1 shRNA or Lox propeptide cDNA in cerebellar cell cultures. Exogenous expression of RelA can block the suppression of Purkinje cell dendritic growth due to excess Lox propeptide. Our data further show that RelA knockdown alters MAP1B and MAP2, two key regulators of Purkinje cell dendritic development.

MAPs promote assembly of tubulin, bind and stabilize microtubules, and form cross-bridge structures between microtubules. MAP1B and MAP2 are among the most abundant neuronal MAPs, and play important roles in neuronal morphogenesis. We confirm that MAP1B and MAP2 are expressed predominantly in Purkinje cell dendrites, relative to Purkinje cell axons (Chauhan and Siegel, 1997). These two MAPs show functional redundancy, since mice with

double knockouts, but not with either single knockout, show inhibited dendritic growth (Teng et al., 2001). We also establish a causal relationship between MAP1B/MAP2 and Purkinje cell dendritic growth by MAP knockdown and overexpression. Thus, our study describes a molecular pathway composed of mutant *Nna1*, excess Lox propeptide, reduced NF-κB RelA, and altered MAP1B and MAP2, which suppresses dendritic growth in developing Purkinje cells. This unusual pathway may be relevant to other cerebellar diseases that primarily affect Purkinje cells.

EXPERIMENTAL PROCEDURES

Animals

We maintained pcd^{Sid} mutants in a congenic C57BL/6J strain, and obtained pcd^{2J}, pcd^{3J} and pcd^{4J} mutants from The Jackson Laboratory. Progeny were generated by either heterozygote × heterozygote crosses, or homozygous female × heterozygous male crosses. The *pcd* genotyping was carried out with *Nna1* genome DNA PCR for pcd^{2J} and pcd^{3J}, Nna1 cDNA sequencing for pcd^{4J}, and Nna1 mRNA RT-PCR for pcd^{Sid}. Adult homozygotes were also identified in segregating litters by the obvious ataxia. The use of animals in the present study was in accordance with NIH-approved institutional guidelines established by Harvard Medical School. All efforts were made to minimize the number of animals used and their suffering.

LCM and microarray analysis

Purified Purkinje and granule cells were isolated from fresh cerebellar tissues of P20 pcd^{Sid} and wild-type littermates by an Arcturus^{XT} LCM instrument (Molecular Devices). PicoPure RNA extraction kit was used to extract total RNA from the cells. WT-Ovation pico RNA amplification kit and FL-Ovation cDNA biotin module V2 kit (NuGEN) were used in succession to prepare enough qualified cDNA for microarray (Affymetrix mouse genome 430 2.0 array).

qPCR and nucleotide sequencing

SYBR Green I-based qPCR was carried out with a DNA engine opticon continuous fluorescence detection system (MJ). For normalization of each sample, GAPDH primers were used to measure the amount of GAPDH cDNA. The data were presented as ratios of measured gene/GAPDH. Some PCR products were verified with 1% agarose gel.

Nucleotide sequence of Nna1 cDNA was analyzed at the BIDMC Sequencing Facility. Samples were electrophoresed, detected and analyzed on a PE/ABI 377 DNA sequencer. Sequence data were analyzed with Gene Runner software and the BLAST program.

Cerebellar cell and slice culture

Mixed cerebellar cells or enriched Purkinje cells from P0 C57BL/6J mouse pups were cultured in serum-free medium for 7–21 DIV; and cerebellar organotypic slices from P7 mouse pups were cultured in serum-containing medium for 7–14 DIV. The cultures were treated with various factors at designated times. Specific antibodies were used to assess Purkinje cell survival, dendritic branchlets, and other cerebellar cells.

Lentiviral vector-based cDNA or shRNA transduction

Omicslink™ expression construct (GeneCopeia), pReceiver-Lv08 with CMV promoter, was used for packaging, transduction and stable integration of Lox, Lox-propeptide, RelA, MAP1B or MAP2 cDNA into genomic DNA of cerebellar cells. Mission™ lentiviral transduction particles (Sigma) containing pLKO.1-puro expression construct with U6 promoter were used to transduce Nna1, Lox, RelA, MAP1B or MAP2 shRNA into cerebellar cells.

Quantification and statistic analysis

Number and proportion of the specific (calbindin, Lox or others) staining positive- and negative-cells were counted from cerebellar cell and slice cultures *in vitro*, or stereologically quantified from a series of representative sequentially-cut cerebellar sagittal sections (40 μm) *in vivo*. Single Purkinje cells in cerebellar cell cultures and grouped Purkinje cells in cerebellar slice cultures or the cerebellar cortices (lobules V-VIII) *in vivo* were randomly selected and imaged by confocal microscopy (Zeiss Axiovert 100M) with a 63x oil objective under optimal conditions (laser power, background and signal threshold). Z series images for each sample acquired by 1 μm optical sectioning were projected onto a 2D image file, and the complete dendritic arborization of Purkinje cells was traced and analyzed with Neurolucida software (MicroBrightField Bioscience). The parameters for dendrite quantification included node number, end number, dendrite length and dendrite distribution (Sholl analysis). The data were presented as the parameter per Purkinje cell in cell cultures (without dendritic tree overlapping between adjacent cells), or as the parameter per field in slice cultures or the cerebellum *in vivo* (with dendritic tree overlapping between adjacent cells). ImageJ software (NIH) was used to quantify immunofluorescence staining images. Quantity I software was used for the quantitative analyses of cDNA and protein bands on gel or film. Comparison between groups, either paired or unpaired as required, was performed with (i) ANOVA and the Student *t* or *t'* test (according to results of the homoscedasticity analysis) for the measurement data, (ii) the *Chi-square* test for enumeration data, (iii) the linear or non-linear regression analysis for correlation data, and (iv) the *Ridit* analysis for ranked data. Results were presented as means ± SD, and differences were considered as significant at $P<0.05$ or very significant at $P<0.01$.

Supplementary Material

Refer to Web version on PubMed Central for supplementary material.

ACKNOWLEDGEMENTS

We thank Kangni Zheng for assistance with cDNA sequencing, Marie G. Joseph with Affymetrix microarray, Veronica J. Peschansky with Neurolucida software, Scott B. Berger with lentiviral particle concentration, and Quanli Yang with statistic analysis. We also thank Professor Philip Leder of the Harvard Medical School Department of Genetics for sharing the ataxic mice. This work was supported in part by NIH R33 CA103056 and the Nancy Lurie Marks Family Foundation (R.L.S.), and the William Randolph Hearst Fund (J.L.).

REFERENCES

Becker EB, Oliver PL, Glitsch MD, Banks GT, Achilli F, Hardy A, Nolan PM, Fisher EM, Davies KE. A point mutation in TRPC3 causes abnormal Purkinje cell development and cerebellar ataxia in moonwalker mice. Proc. Natl. Acad. Sci. U. S. A. 2009; 106:6706–6711. [PubMed: 19351902]

Bedard K, Szabo E, Michalak M, Opas M. Cellular functions of endoplasmic reticulum chaperones calreticulin, calnexin, and ERp57. Int. Rev. Cytol. 2005; 245:91–121. [PubMed: 16125546]

Buchinger B, Spitzer S, Karlic H, Klaushofer K, Varga F. Lysyl oxidase (LOX) mRNA expression and genes of the differentiated osteoblastic phenotype are upregulated in human osteosarcoma cells by suramin. Cancer Lett. 2008; 265:45–54. [PubMed: 18374478]

Chauhan N, Siegel G. Age-dependent organotypic expression of microtubule-associated proteins (MAP1, MAP2, and MAP5) in rat brain. Neurochem. Res. 1997; 22:713–719. [PubMed: 9178955]

Dusart I, Guenet JL, Sotelo C. Purkinje cell death: differences between developmental cell death and neurodegenerative death in mutant mice. Cerebellum. 2006; 5:163–173. [PubMed: 16818391]

Erler JT, Bennewith KL, Nicolau M, Dornhöfer N, Kong C, Le QT, Chi JT, Jeffrey SS, Giaccia AJ. Lysyl oxidase is essential for hypoxia-induced metastasis. Nature. 2006; 440:1222–1226. [PubMed: 16642001]

Ford GD, Ford BD, Steele EC Jr, Gates A, Hood D, Matthews MAB, Mirza S, MacLeish PR. Analysis of transcriptional profiles and functional clustering of global cerebellar gene expression in PCD3J mice. Biochem. Biophys. Res. Commun. 2008; 377:556–561. [PubMed: 18930027]

Gilad GM, Kagan HM, Gilad VH. Lysyl oxidase, the extracellular matrix-forming enzyme, in rat brain injury sites. Neurosci. Lett. 2001; 310:45–48. [PubMed: 11524154]

Gilad GM, Kagan HM, Gilad VH. Evidence for increased lysyl oxidase, the extracellular matrix-forming enzyme, in Alzheimer's disease brain. Neurosci. Lett. 2005; 376:210–214. [PubMed: 15721223]

Greene LA, Liu DX, Troy CM, Biswas SC. Cell cycle molecules define a pathway required for neuron death in development and disease. Biochim. Biophys. Acta. 2007; 1772:392–401. [PubMed: 17229557]

Guo Y, Pischon N, Palamakumbura AH, Trackman PC. Intracellular distribution of the lysyl oxidase propeptide in osteoblastic cells. Am. J. Physiol. Cell Physiol. 2007; 292:C2095–C2102. [PubMed: 17287363]

Gutierrez H, Hale VA, Dolcet X, Davies A. NF-kappaB signaling regulates the growth of neural processes in the developing PNS and CNS. Development. 2005; 132:1713–1726. [PubMed: 15743881]

Hirai H. Progress in transduction of cerebellar Purkinje cells in vivo using viral vectors. Cerebellum. 2008; 7:273–278. [PubMed: 18418690]

Hurtado PA, Vora S, Sume SS, Yang D, St Hilaire C, Guo Y, Palamakumbura AH, Schreiber BM, Ravid K, Trackman PC. Lysyl oxidase propeptide inhibits smooth muscle cell signaling and proliferation. Biochem. Biophys. Res. Commun. 2008; 366:156–161. [PubMed: 18060869]

Kapfhammer JP. Cellular and molecular control of dendritic growth and development of cerebellar Purkinje cells. Prog. Histochem. Cytochem. 2004; 39:131–182. [PubMed: 15580762]

Kyuhou S, Kato N, Gemba H. Emergence of endoplasmic reticulum stress and activated microglia in Purkinje cell degeneration mice. Neurosci. Lett. 2006; 396:91–96. [PubMed: 16356646]

Landis SC, Mullen RJ. The development and degeneration of Purkinje cells in pcd mutant mice. J. Comp. Neurol. 1978; 177:125–143. [PubMed: 200636]

Li J, Imitola J, Snyder EY, Sidman RL. Neural stem cells rescue nervous Purkinje neurons by restoring molecular homeostasis of tissue plasminogen activator and downstream targets. J. Neurosci. 2006a; 26:7839–7848. [PubMed: 16870729]

Li J, Ma Y, Teng YD, Zheng K, Vartanian TK, Snyder EY, Sidman RL. Purkinje neuron degeneration in nervous (nr) mutant mice is mediated by a metabolic pathway involving excess tissue plasminogen activator. Proc. Natl. Acad. Sci. U. S. A. 2006b; 103:7847–7852. [PubMed: 16682647]

Li PA, He Q, Cao T, Yong G, Szauter KM, Fong KS, Karlsson J, Keep MF, Csiszar K. Up-regulation and altered distribution of lysyl oxidase in the central nervous system of mutant SOD1 transgenic

mouse model of amyotrophic lateral sclerosis. Brain Res. Mol. Brain Res. 2004; 120:115–122. [PubMed: 14741400]

Lucero HA, Kagan HM. Lysyl oxidase: an oxidative enzyme and effector of cell function. Cell Mol. Life Sci. 2006; 63:2304–2316. [PubMed: 16909208]

Mäki JM. Lysyl oxidases in mammalian development and certain pathological conditions. Histol. Histopathol. 2009; 24:651–660. [PubMed: 19283672]

Meffert MK, Chang JM, Wiltgen BJ, Fanselow MS, Baltimore D. NF-kappa B functions in synaptic signaling and behavior. Nat. Neurosci. 2003; 6:1072–1078. [PubMed: 12947408]

Min C, Kirsch KH, Zhao Y, Jeay S, Palamakumbura AH, Trackman PC, Sonenshein GE. The tumor suppressor activity of the lysyl oxidase propeptide reverses the invasive phenotype of Her-2/neu-driven breast cancer. Cancer Res. 2007; 67:1105–1112. [PubMed: 17283144]

Mullen RJ. Site of pcd gene action and Purkinje cell mosaicism in cerebella of chimaeric mice. Nature. 1977; 270:245–247. [PubMed: 593342]

Palamakumbura AH, Jeay S, Guo Y, Pischon N, Sommer P, Sonenshein GE, Trackman PC. The propeptide domain of lysyl oxidase induces phenotypic reversion of ras-transformed cells. J. Biol. Chem. 2004; 279:40593–40600. [PubMed: 15277520]

Palamakumbura AH, Vora SR, Nugent MA, Kirsch KH, Sonenshein GE, Trackman PC. Lysyl oxidase propeptide inhibits prostate cancer cell growth by mechanisms that target FGF-2-cell binding and signaling. Oncogene. 2009; 28:3390–3400. [PubMed: 19597471]

Payne SL, Hendrix MJ, Kirschmann DA. Paradoxical roles for lysyl oxidases in cancer - a prospect. J. Cell. Biochem. 2007; 101:1338–1354. [PubMed: 17471532]

Poulain FE, Chauvin S, Wehrlé R, Desclaux M, Mallet J, Vodjdani G, Dusart I, Sobel A. SCLIP is crucial for the formation and development of the Purkinje cell dendritic arbor. J. Neurosci. 2008; 28:7387–7398. [PubMed: 18632943]

Rodríguez C, Martínez-González J, Raposo B, Alcudia JF, Guadall A, Badimon L. Regulation of lysyl oxidase in vascular cells: lysyl oxidase as a new player in cardiovascular diseases. Cardiovasc. Res. 2008; 79:7–13. [PubMed: 18469024]

Rossi F, Tempia F. Unraveling the Purkinje neuron. Cerebellum. 2006; 5:75–76. [PubMed: 16818381]

Royuela M, Rodríguez-Berriguete G, Fraile B, Paniagua R. TNF-alpha/ IL-1/NF-kappaB transduction pathway in human cancer prostate. Histol. Histopathol. 2008; 23:1279–1290. [PubMed: 18712680]

Sarna JR, Hawkes R. Patterned Purkinje cell death in the cerebellum. Prog. Neurobiol. 2003; 70:473–507. [PubMed: 14568361]

Sawada Y, Kajiwara G, Iizuka A, Takayama K, Shuvaev AN, Koyama C, Hirai H. High transgene expression by lentiviral vectors causes maldevelopment of Purkinje cells in vivo. Cerebellum. 2010 Feb.23 [Epub ahead of print].

Shima Y, Kengaku M, Hirano T, Takeichi M, Uemura T. Regulation of dendritic maintenance and growth by a mammalian 7-pass transmembrane cadherin. Dev. Cell. 2004; 7:205–216. [PubMed: 15296717]

Sirzen-Zelenskaya A, Zeyse J, Kapfhammer JP. Activation of class I metabotropic glutamate receptors limits dendritic growth of Purkinje cells in organotypic slice cultures. Eur. J. Neurosci. 2006; 24:2978–2986. [PubMed: 17156359]

Sotelo C, Dusart I. Intrinsic versus extrinsic determinants during the development of Purkinje cell dendrites. Neuroscience. 2009; 162:589–600. [PubMed: 19166910]

Szauter KM, Cao T, Boyd CD, Csiszar K. Lysyl oxidase in development, aging and pathologies of the skin. Pathol. Biol. (Paris). 2005; 53:448–456. [PubMed: 16085123]

Tabata T, Sawada S, Araki K, Bono Y, Furuya S, Kano M. A reliable method for culture of dissociated mouse cerebellar cells enriched for Purkinje neurons. J. Neurosci. Methods. 2000; 104:45–53. [PubMed: 11163410]

Takayama K, Torashima T, Horiuchi H, Hirai H. Purkinje-cell-preferential transduction by lentiviral vectors with the murine stem cell virus promoter. Neurosci. Lett. 2008; 443:7–11. [PubMed: 18675313]

Teng J, Takei Y, Harada A, Nakata T, Chen J, Hirokawa N. Synergistic effects of MAP2 and MAP1B knockout in neuronal migration, dendritic outgrowth, and microtubule organization. J. Cell Biol. 2001; 155:65–76. [PubMed: 11581286]

Torashima T, Yamada N, Itoh M, Yamamoto A, Hirai H. Exposure of lentiviral vectors to subneutral pH shifts the tropism from Purkinje cell to Bergmann glia. Eur. J. Neurosci. 2006; 24:371–380. [PubMed: 16836635]

Wang T, Morgan JI. The Purkinje cell degeneration (pcd) mouse: an unexpected molecular link between neuronal degeneration and regeneration. Brain Res. 2007; 1140:26–40. [PubMed: 16942761]

Wong RO, Ghosh A. Activity-dependent regulation of dendritic growth and patterning. Nat. Rev. Neurosci. 2002; 3:803–812. [PubMed: 12360324]

Wu M, Min C, Wang X, Yu Z, Kirsch KH, Trackman PC, Sonenshein GE. Repression of BCL2 by the tumor suppressor activity of the lysyl oxidase propeptide inhibits transformed phenotype of lung and pancreatic cancer cells. Cancer Res. 2007; 67:6278–6285. [PubMed: 17616686]

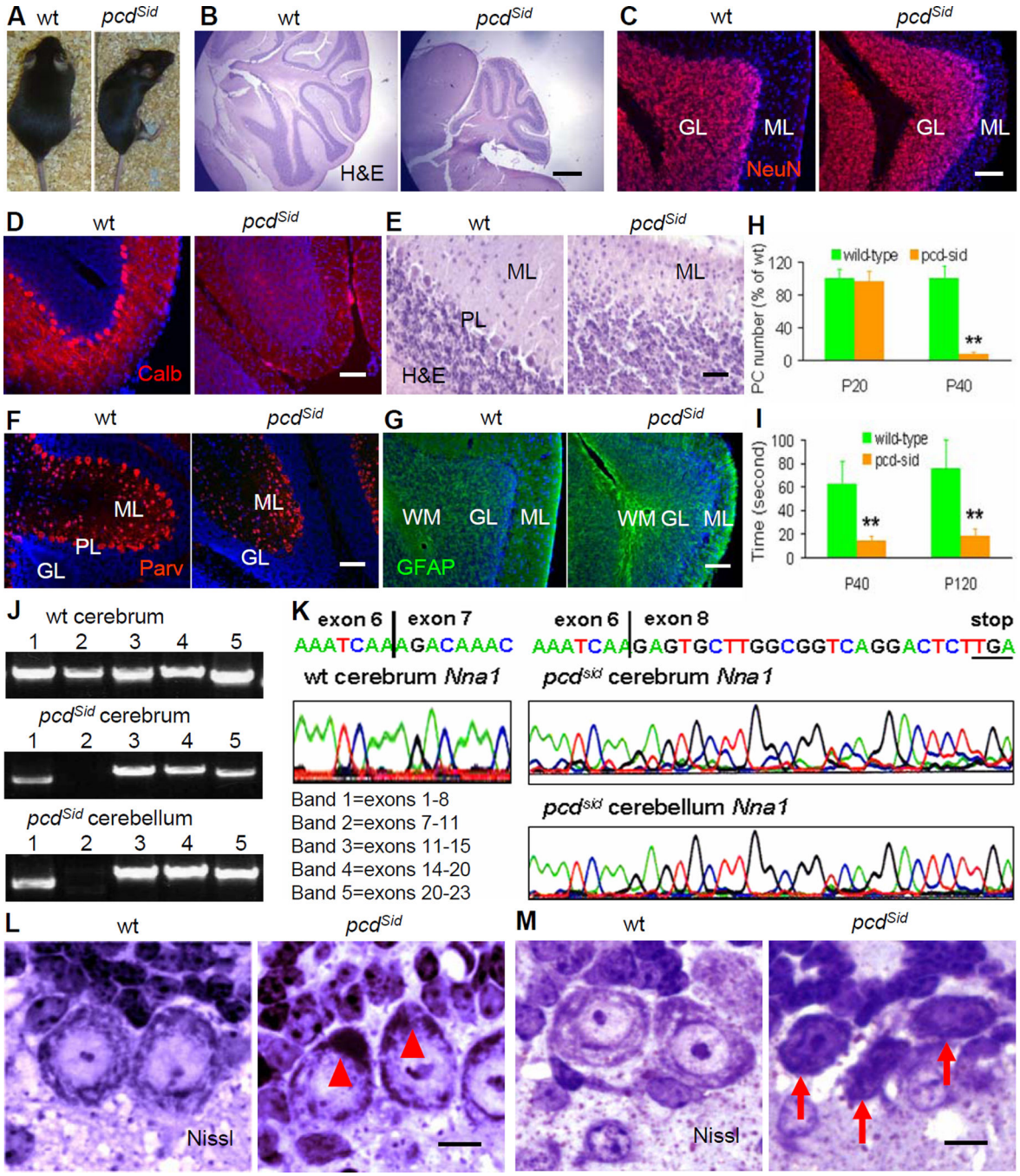

Figure 1. Characterization of cerebellar histopathology, motor ability and *Nna1* mutation in *pcd*^{Sid} mutant mice

(A) Compared to wild-type (wt) mouse, adult P120 *pcd*^{Sid} mutant was smaller and showed motor incoordination.

(B) Hematoxylin and eosin (H&E)-stained sagittal section showed an atrophic cerebellum in P120 *pcd*^{Sid} mutant. Scale bar: 500 μm.

(C) Neuron-specific nuclear protein (NeuN)-stained granule cells (red) in the granular layer (GL) were slightly decreased, while the molecular layer (ML) was obviously reduced in P120 *pcd*^{Sid} cerebellar cortex. DAPI stained cell nuclei (blue). Scale bar: 50 μm.
(D) Calbindin (Calb)-stained Purkinje cells (red) were totally lost in P60 *pcd*^{Sid} cerebellar cortex. Scale bar: 50 μm.
(E) The Purkinje cell body layer (PL) was disappeared, and the ML was shrunk in P60 *pcd*^{Sid} cerebellar cortex. Scale bar: 25 μm.
(F) Parvalbumin (Parv)-stained interneurons (red) in the ML showed no obvious changes, while Parv-stained Purkinje cell bodies at the PL were disappeared in P60 *pcd*^{Sid} cerebellar cortex. Scale bar: 50 μm.
(G) Glial fibrillary acidic protein (GFAP)-stained astrocytes (green) were obviously increased in the white matter (WM) of P120 *pcd*^{Sid} cerebellar cortex. Scale bar: 50 μm.
(H) Quantification of Purkinje cells in P20 and P40 mouse cerebella. Values represented means ± SD; n = 6–8; compared to wild-type control: **, $P<0.01$.
(I) Quantification of rotarod test showing motor ability of P40 and P120 mice. n = 4–5.
(J) RT-PCR detection of Nna1 cDNA from P120 wt and *pcd*^{Sid} cerebra and cerebella. Bands 1–5 represented 5 fragments amplified by 5 pairs of primers covering all 23 exons in mouse Nna1 cDNA. Band 1 contained exons 1–8, and its smaller molecular weight in *pcd*^{Sid} samples indicated a partial deletion in that region. Since band 2 represented exons 7–11, its disappearance in *pcd*^{Sid} samples suggested a possible mutation in exon 7 and/or exon 11.
(K) cDNA sequencing disclosed a deletion of the entire exon 7 (209 bp), producing a new stop codon (TGA) in exon 8 of Nna1 cDNA in P120 *pcd*^{Sid} cerebrum and cerebellum.
(L) P14 *pcd*^{Sid} Purkinje cells contained a polyribosome mass in the basal region (arrowheads). Nissl, Nissl staining. Scale bar: 10 μm.
(M) Some P20 *pcd*^{Sid} Purkinje cells started to display dark type of apoptotic death with nuclear condensation and cytoplasm shrinkage (arrows). Scale bar: 10 μm.

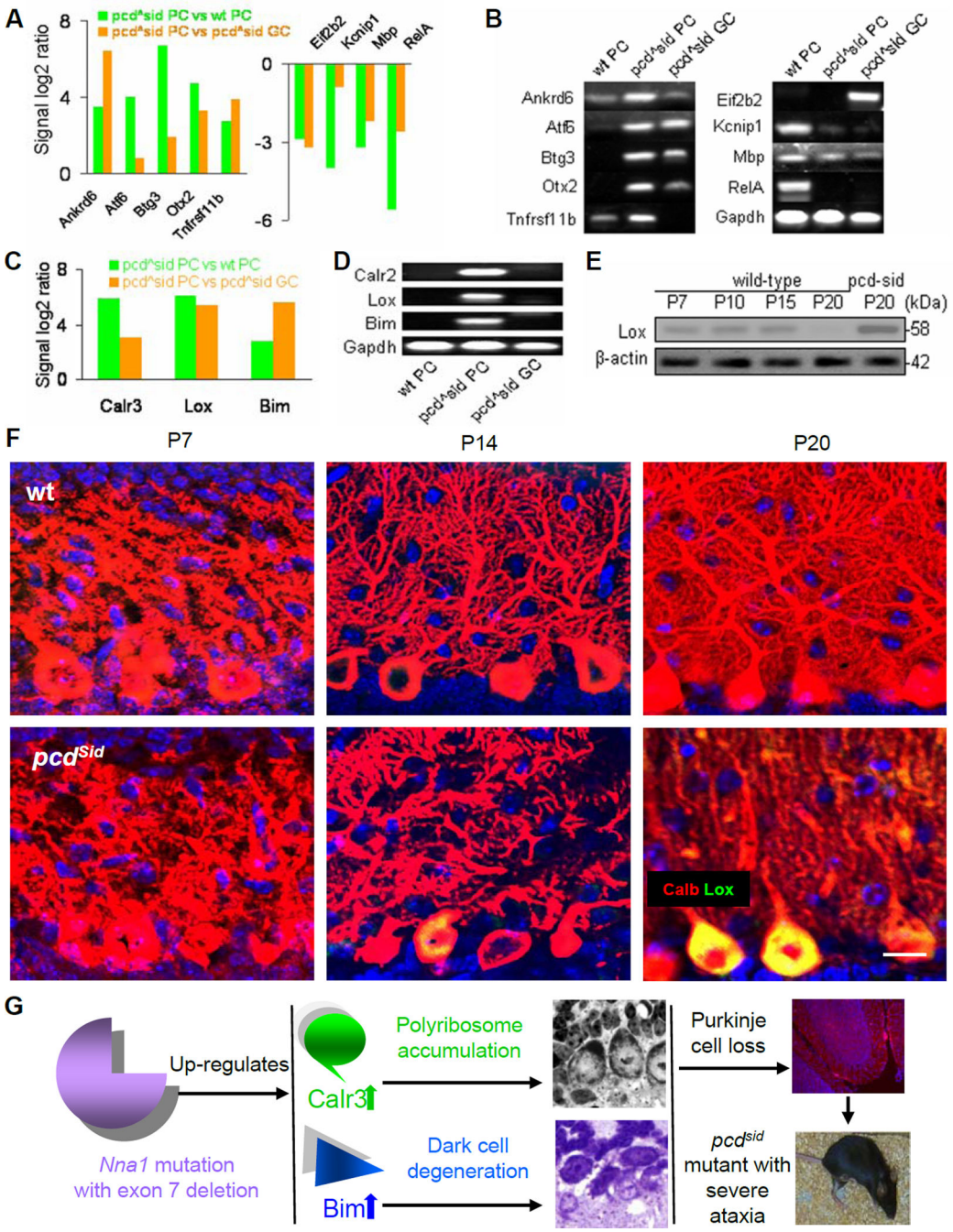

Figure 2. Candidate molecules identified by LCM, microarray, qPCR and protein assays for pathological process in young *pcd*^{Sid} Purkinje cells

(A) Microarray analysis showed several up-regulated (left) or down-regulated (right) genes in P20 LCM-isolated *pcd*^{Sid} PC, compared to wt PC and *pcd*^{Sid} GC. *pcd*^{Sid} PC and *pcd*^{Sid} GC were from same mouse, and wild-type (wt) cells and *pcd*^{Sid} cells were from littermates.

(B) qPCR verified the microarray results in Figure 2A. Gapdh served as an internal control.

(C) Microarray analysis disclosed remarkable up-regulation of Calr3, Lox and Bim in P20 *pcd*^{Sid} PC, compared to wt PC and *pcd*^{Sid} GC.

(D) qPCR verified the microarray results for Calr3, Lox and Bim.

(E) Western blot showed very low levels of Lox protein in P7, P10, P15 and P20 wild-type cerebella and an increased level in P20 *pcd*^{Sid} cerebellum. β-actin served as a loading control.

(F) Immunohistochemical images showed postnatal development of Purkinje cell dendrites in P7, P14 and P20 wt (upper) and *pcd*^{Sid} (lower) cerebellar cortices. The increased Lox staining (green) in P20 *pcd*^{Sid} Purkinje cell bodies (Calb, red) gave a net yellow color, and was concurrent with the reduced dendritic branching (Calb, red). Calb, calbindin staining. DAPI stained cell nuclei (blue). Scale bar: 12 μm.

(G) Schematics summarizing the major pathological processes leading to *pcd*^{Sid} Purkinje cells death. *Nna1* mutation triggered abnormal protein metabolism and dark type of apoptosis, which finally resulted in loss of most Purkinje cell and severe ataxia in *pcd*^{Sid} mutant mice.

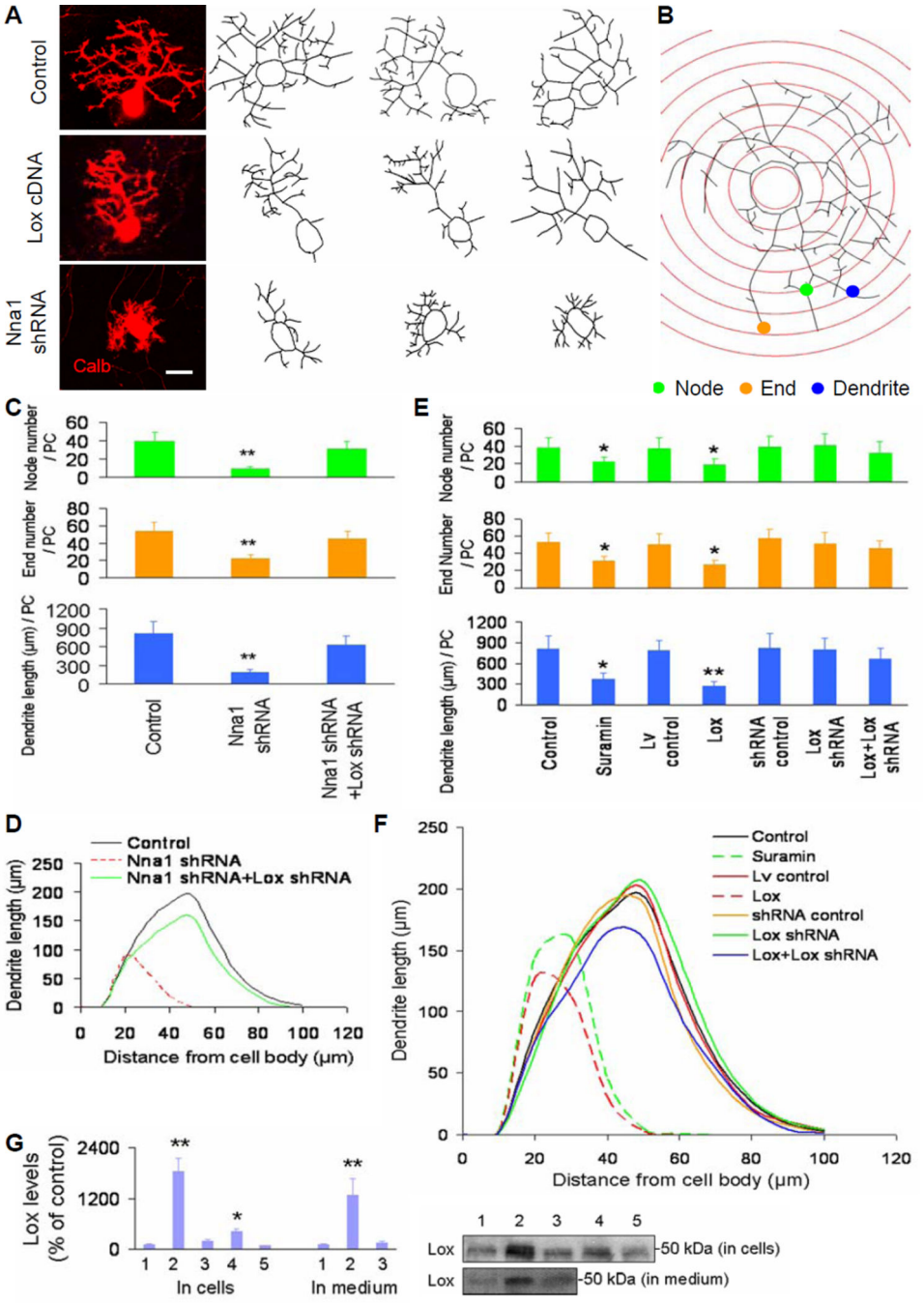

Figure 3. Purkinje cell dendritic growth in cerebellar cell cultures transduced by Nna1 shRNA, Lox cDNA and Lox shRNA

(A) Representative images of cultured Purkinje cells stained by calbindin (Calb, left) and traced with Neurolucida (right). The images were obtained by confocal microscopy (63x, oil objective) for dendrite tracing. Scale bar: 15 μm.

(B) Representative schematic Sholl diagram showed parameters of node (green dot), end (orange dot) and dendrite (blue dot) for quantification of Purkinje cell dendritic trees. The distance between adjacent concentric circles was 10 μm.

(C and E) Quantitative analyses showed total node or end number and total dendrite length per Purkinje cell (PC) at 14 DIV in cerebellar cell cultures. Control, control cDNA or shRNA; Lox, Lox cDNA; Lv, lentiviral vector. Values represented means ± SD; n = 6–10; compared to control: *, $P<0.05$ or **, $P<0.01$.

(D and F) Sholl analyses showed total length of Purkinje cell dendrites within each concentric circle (0–10 μm, 10–20 μm, … 90–100 μm) at 14 DIV in cerebellar cell cultures. Each curve area represented an average value of total Purkinje cell dendrite length in each treatment. Peak values positively correlated with dendritic density.

(G) Western blot results were quantified with Quality I software, and showed Lox protein levels at 14 DIV in both cultured cells and culture medium. 1: Control; 2: Lox cDNA; 3: Lox cDNA+Lox shRNA; 4: Nna1 shRNA; 5: Nna1 shRNA+Lox shRNA. n = 3.

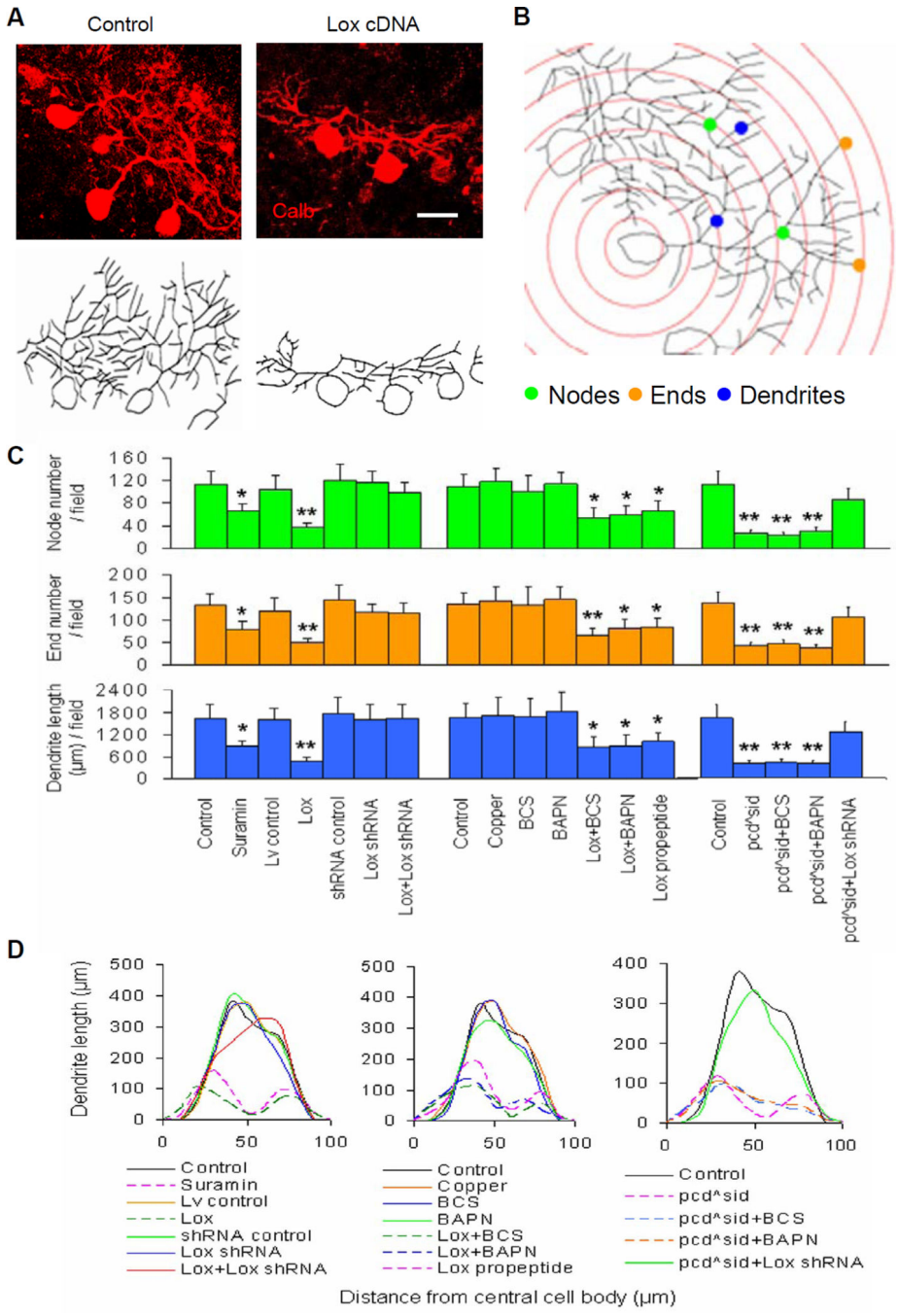

Figure 4. Quantification of Purkinje cell dendritic trees in wild-type and *pcd*^{Sid} cerebellar slice cultures

(A) Representative images of Purkinje cells in organotypic slice cultures stained by calbindin (Calb, upper) and traced with Neurolucida (lower). Cultures were photographed by confocal microscopy (63x, oil objective) for dendrite tracing. Scale bar: 20 μm.

(B) Representative schematic Sholl diagram showed parameters as in Figure 3B.

(C) Quantitative analyses showed total node or end number and total dendrite length per field at the 14th day (P7 + 7 DIV) in wild-type (left and middle) and *pcd*^{Sid} (right) cerebellar slice cultures after various treatments. Control, control cDNA or shRNA; Lox, Lox cDNA;

Lv, lentiviral vector. BCS and BAPN are Lox enzymatic inhibitors. Values represented means ± SD; n = 4–8; compared to control: *, $P<0.05$ or **, $P<0.01$.
(D) Sholl analysis showed total length of Purkinje cell dendrites within each concentric circle (0–10 μm, 10–20 μm, … 90–100 μm) at the 14th day (P7 + 7 DIV) in wild-type (left and middle) and *pcd*^{Sid} (right) cerebellar slice cultures after various treatments. Each curve area represented an average value of total Purkinje cell dendrite length in each treatment. Peak values positively correlated with dendritic density.

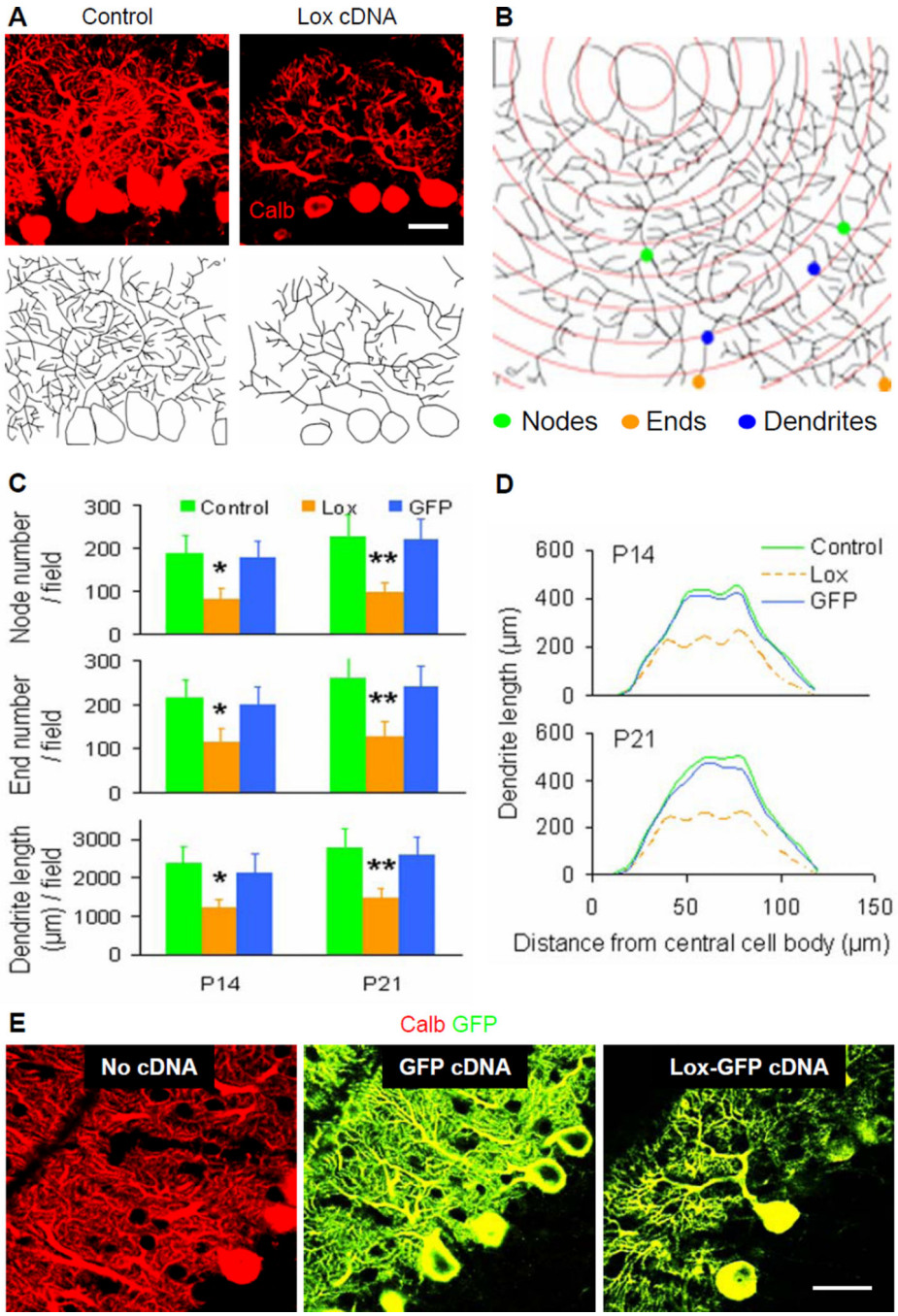

Figure 5. Effects of lentiviral vector-based Lox cDNA transduction on Purkinje cell dendritic development *in vivo*

(A) Representative fields of calbindin (Calb)-stained (upper) and Neurolucida-traced (lower) Purkinje cells. Serial stained cerebellar sections (40 μm in thick) were photographed by confocal microscopy (63x, oil objective) for dendrite tracing. Scale bar: 20 μm.

(B) Representative schematic Sholl diagram showed parameters as in Figure 3B.

(C) Quantitative analyses showed total node or end number and total dendrite length per field in P14 (left) and P21 (right) cerebellar cortices. Control, control cDNA; Lox, Lox

cDNA; GFP, GFP cDNA. Values represented means ± SD; n = 4–6; compared to control: *, $P<0.05$ or **, $P<0.01$.

(D) Sholl analysis showed total length of Purkinje cell dendrites within each concentric circle (0–10 μm, 10–20 μm, … 110–120 μm) in P14 (upper) and P21 (lower) cerebellar cortices. Each curve area represented an average value of total Purkinje cell dendrite length in each treatment. Peak values positively correlated with dendritic density.

(E) No cDNA-, GFP cDNA- and Lox-GFP cDNA-transduced Purkinje cells (GFP tag, green) were stained with calbindin (Calb, red) for cell bodies and dendrites. GFP itself alone did not affect Purkinje cell dendrites, but Lox over-expression suppressed obviously Purkinje cell dendritic development. Scale bar: 20 μm.

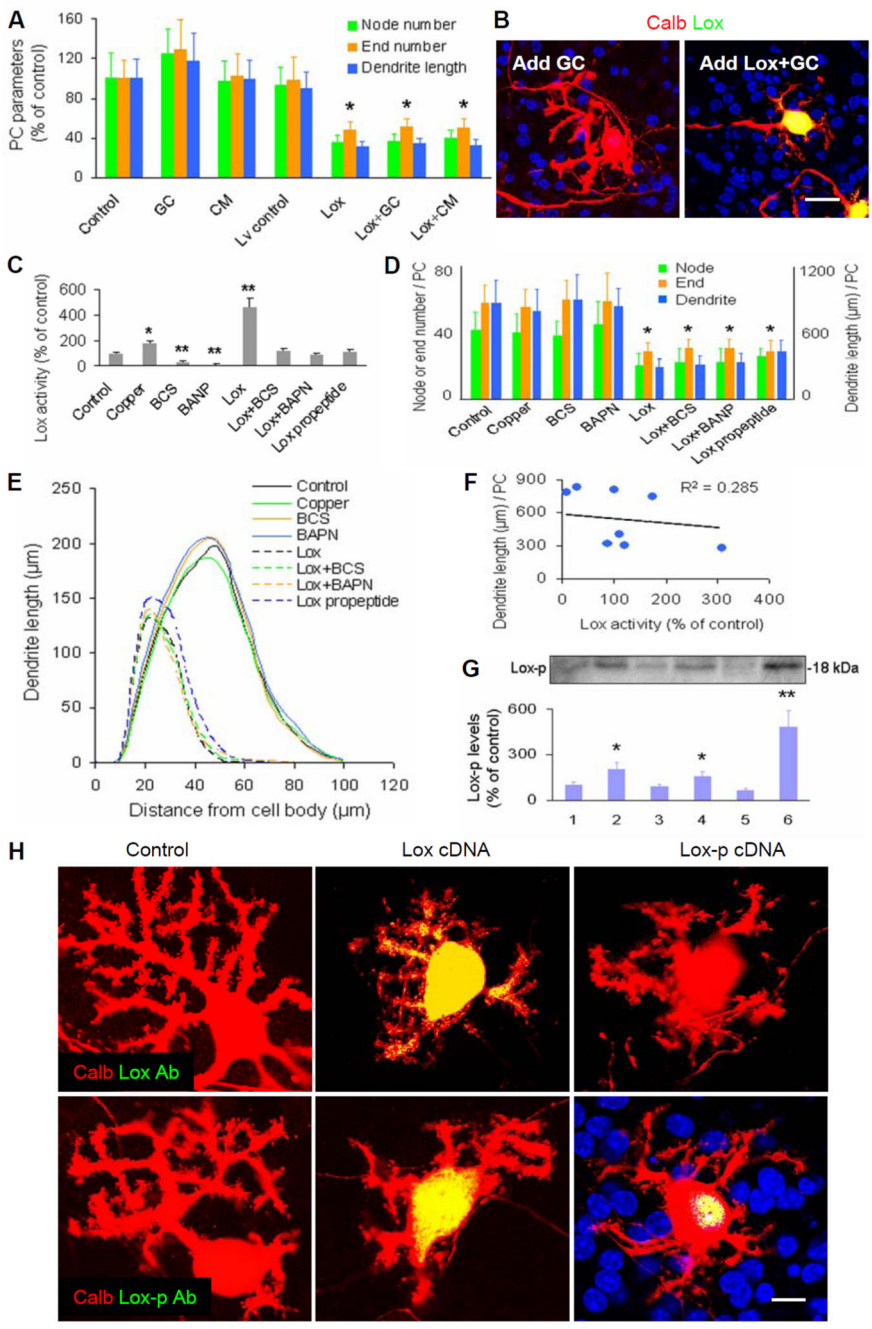

Figure 6. Roles of Lox enzymatic regulators and intranuclear Lox propeptide (without enzymatic activity) in cerebellar Purkinje cell cultures

(A) Total relative number of nodes or ends, and total relative dendrite length per Purkinje cell at 14 DIV in enriched Purkinje cell (PC) cultures. Control, control cDNA or shRNA; Lox, Lox cDNA; Lv, lentiviral vector; GC, enriched granule cells; CM, conditioned medium from cerebellar mixed cell cultures. Values represented means ± SD; n = 6–8; compared to control: *, $P<0.05$ or **, $P<0.01$.

(B) Representative images of cultured Purkinje cells stained by calbindin (Calb, red) and Lox (green). Addition of granule cells (GC) neither affected Purkinje cell dendrites (left),

nor rectified Lox cDNA-suppressed Purkinje cell dendritic growth (right). DAPI stained mainly granule cell nuclei (blue). Scale bar: 20 μm.

(C) Lox enzymatic activities at 14 DIV in cerebellar cell cultures. BCS and BAPN were Lox enzymatic inhibitors. Lox propeptide, Lox propeptide cDNA. n = 4–6.

(D) Quantitative analyses showed total node or end number and total dendrite length per PC at 14 DIV in cerebellar cell cultures. n = 6–10.

(E) Sholl analyses showed total length of PC dendrites within each concentric circle (0–10 μm, 10–20 μm, … 90–100 μm) at 14 DIV in cerebellar cell cultures. Each curve area represented an average value of total PC dendrite length in each treatment. Peak values positively correlated with dendritic density.

(F) No significant correlation between Lox enzymatic activity and PC dendrite length at 14 DIV in cerebellar cell cultures. $R^2 = 0.285$ ($P>0.05$).

(G) Western blot results were quantified with Quality I software, and showed Lox propeptide (Lox-p) levels at 14 DIV in cerebellar cell cultures. 1: Control; 2: Lox cDNA; 3: Lox cDNA+Lox shRNA; 4: Nna1 shRNA; 5: Nna1 shRNA+Lox shRNA; 6: Lox propeptide cDNA. n = 4–6.

(H) Immunostaining showed intracellular or intranuclear localization of Lox and Lox-p in Lox cDNA- or Lox-p cDNA-transduced Purkinje cells of cerebellar cell cultures. The Lox antibody (Lox Ab, green) against C-terminal of Lox could detect entire Lox and/or Lox enzyme (upper), and the Lox-p antibody (Lox-p Ab, green) against N-terminal of Lox could detect entire Lox and/or Lox-p (lower). Scale bar: 10 μm.

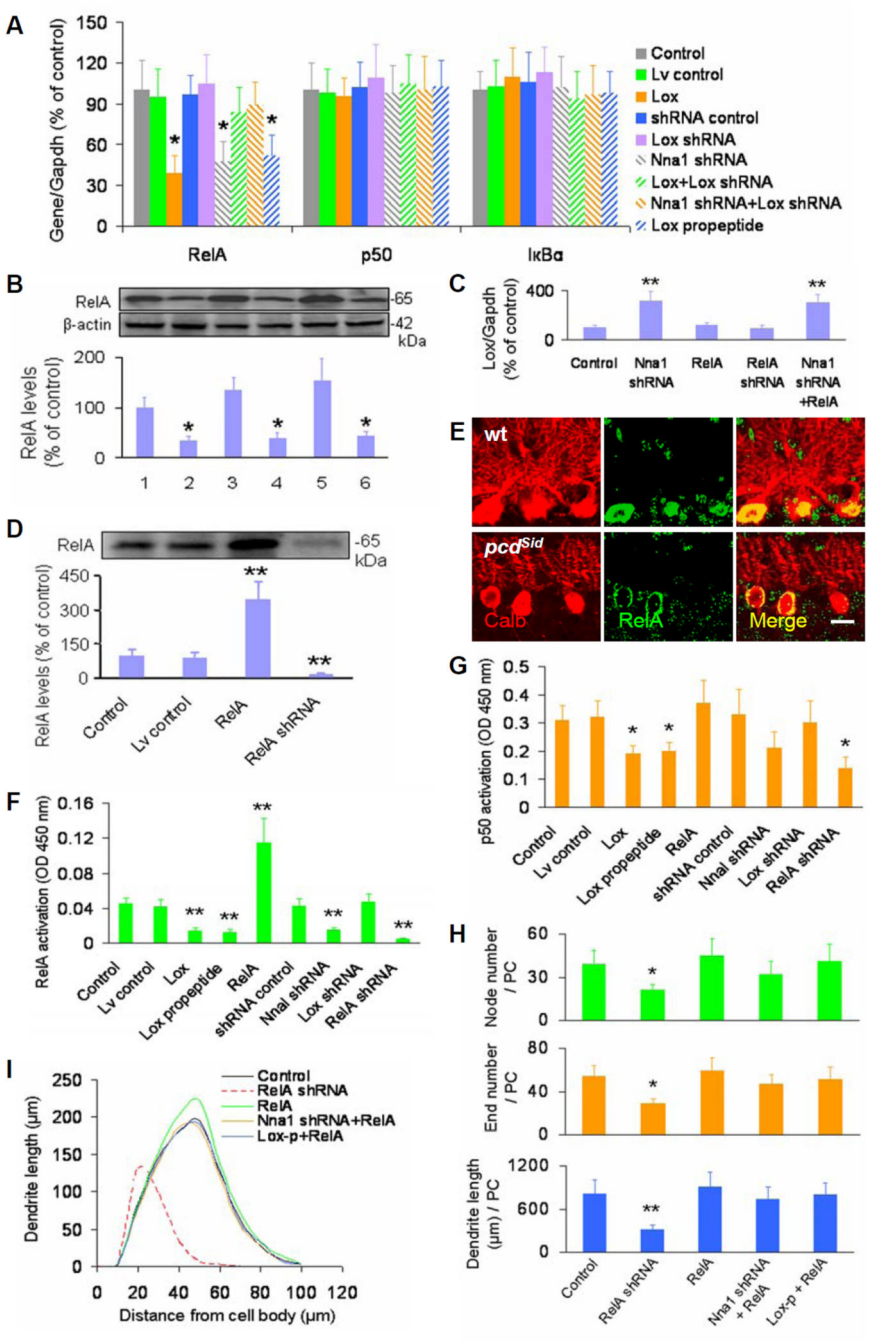

Figure 7. Roles of reduced NF-κB RelA in mutant *Nna1*- and excess Lox propeptide-suppressed Purkinje cell dendritic growth

(A) qPCR results showed mRNA levels of RelA, p50 and IκBα in the NF-κB family at 14 DIV in cerebellar cell cultures. Control, control cDNA or shRNA; Lox, Lox cDNA; Lox propeptide, Lox propeptide cDNA; Lv, lentiviral vector. Gapdh served as an internal control. Values represented means ± SD; n = 5–6; compared to control: *, $P<0.05$ or **, $P<0.01$.

(B) Western blot results were quantified with Quality I software, and showed RelA protein levels at 14 DIV in cerebellar cell cultures. β-actin served as a loading control. 1: Control; 2: Lox cDNA; 3: Lox cDNA+Lox shRNA; 4: Nna1 shRNA; 5: Nna1 shRNA+Lox shRNA; 6: Lox propeptide cDNA. n = 3.

(C) qPCR results showed Lox mRNA levels at 14 DIV in cerebellar cell cultures. RelA, RelA cDNA. n = 5.

(D) Western blot results were quantified with Quality I software, and showed RelA protein levels at 14 DIV in cerebellar cell cultures transduced by RelA cDNA or shRNA. n = 3.

(E) Immunohistochemical images showed RelA protein distribution in Purkinje cells of P20 wild-type (wt; upper) and *pcd*^{Sid} (lower) cerebellar cortices *in vivo*. The decreased RelA staining (green) in *pcd*^{Sid} Purkinje cell bodies (Calb, red) was concurrent with the reduced dendritic branching (Calb, red). Calb, calbindin staining. Scale bar: 12 μm.

(F and G) ELISA assay detected NF-κB RelA (F) or p50 (G) transactivation at 14 DIV in nuclear extracts from cultured Purkinje cells. n = 4.

(H) Quantitative analyses showed total node or end number and total dendrite length per Purkinje cell (PC) at 14 DIV in cerebellar cell cultures transduced by RelA cDNA or shRNA. Lox-p, Lox propeptide cDNA. n = 5–6.

(I) Sholl analysis showed total length of Purkinje cell dendrites within each concentric circle (0–10 μm, 10–20 μm, … 90–100 μm) at 14 DIV in cerebellar cell cultures transduced by RelA cDNA or shRNA. Each curve area represented an average value of total Purkinje cell dendrite length in each treatment. Peak values positively correlated with dendritic density.

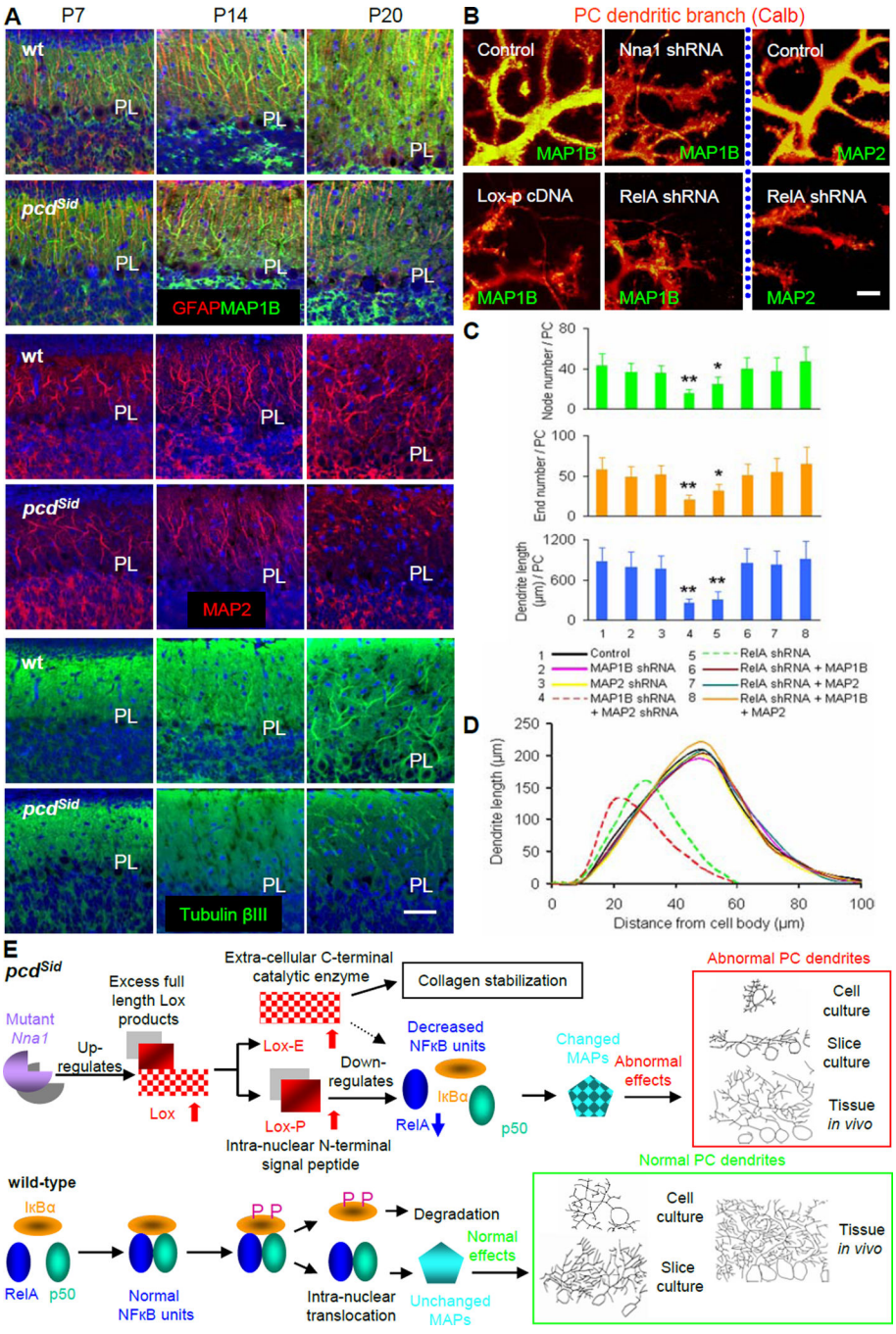

Figure 8. Regulatory roles MAP1B and MAP2 in Purkinje cell dendritic growth

(A) Representative immunohistochemical images showed the spatial and temporal distribution of MAPs and microtubules in P7, P14 and P20 wild-type (wt; upper) and *pcd*^{Sid} (lower) cerebellar cortices *in vivo*. Decreased staining with MAP1B (green), MAP2 (red) or Tubulin βIII (green) was concurrent with Purkinje cell dendritic underdevelopment in P20 *pcd*^{Sid} mutant cerebellar cortices. Glial fibrillary acidic protein (GFAP) stained Bergmann glial cell processes (red), and DAPI stained cell nuclei (blue). PL, the Purkinje cell body layer. Scale bar: 30 μm.

(B) Representative images of double immunostaining with calbindin (Calb, red) and MAPs (green) for cultured Purkinje cell dendritic branchlets. Transduction with Nna1 shRNA, Lox propeptide (Lox-p) cDNA or RelA shRNA significantly decreased MAP1B (left and middle) or MAP2 (right) distribution, and suppressed Purkinje cell dendritic growth. Scale bar: 5 μm.

(C) Quantitative analyses showed total node or end number and total dendrite length per Purkinje cell (PC) at 14 DIV in cerebellar cell cultures transduced by MAP cDNA or shRNA. MAP1B, MAP1B cDNA; MAP2, MAP2 cDNA. Values represented means ± SD; n = 4–5; compared to control: *, $P<0.05$ or **, $P<0.01$.

(D) Sholl analysis showed total length of Purkinje cell dendrites within each concentric circle (0–10 μm, 10–20 μm, … 90–100 μm) at 14 DIV in cerebellar cell cultures transduced by MAP cDNA or shRNA. Each curve area represented an average value of total Purkinje cell dendrite length in each treatment. Peak values positively correlated with dendritic density.

(E) Schematics summarizing the unusual molecular pathway: *Nna1* mutation increased intranuclear Lox propeptide, which in turn reduced NF-κB RelA, altered MAPs, and suppressed Purkinje cell (PC) dendritic growth in pcd^{Sid} mutant cerebellum.